

# Directional Analysis of Digitized 3D Images by Configuration Counts

P. Gutkowski, E. B. V. Jensen and M. Kiderlen



# Directional Analysis of Digitized 3D Images by Configuration Counts

This Thiele Research Report is also Research Report number 439 in the Stochastics Series at Department of Mathematical Sciences, University of Aarhus, Denmark.



# Directional Analysis of Digitized 3D Images by Configuration Counts

P. Gutkowski\*    E.B.V. Jensen†    M. Kiderlen‡

## Abstract

A method for estimating the oriented rose of normal directions of a three dimensional set  $Z$  from a digitization of  $Z$ , i.e. a voxel image, is presented. It is based on counts of informative configurations in  $n \times n \times n$  voxel cubes. An algorithm for finding all informative configurations is proposed and an estimation procedure is described in detail for the case  $n = 2$ . The presented method is a 3D version of a method of estimating the oriented rose of binary planar images using  $n \times n$  configurations. A new feature is the design-based approach, being more appropriate for biomedical image analysis than the formerly applied model-based approach.

*Keywords:* configuration; design-based approach; normal measure; orientation distribution; oriented rose; 3D binary image

## 1 Introduction

An analysis of various biological structures often aims to estimate their anisotropy. It can be expressed quantitatively using the *orientation distribution*, known also as the *oriented rose of normal directions*. The oriented rose is the distribution of the outer unit normal at a uniform random point on the boundary of the structure.

Contemporary scanning techniques allow to produce 3D raster images of such structures. In the present paper a method of estimating the oriented rose of normal directions of a discretized spatial structure is presented using  $2 \times 2 \times 2$  configurations of voxels.

For the planar case, an estimation method for the oriented rose of normal directions from binary images using  $2 \times 2$  configurations of pixels has been presented

---

\*Medical Electronics Division, Institute of Electronics, Technical University of Lodz, Wolczanska 223, 90-924 Lodz, Poland

†Department of Mathematical Sciences, University of Aarhus, Ny Munkegade, DK-8000 Aarhus C, Denmark

‡Mathematical Institute II, University of Karlsruhe, D-76128 Karlsruhe, Germany

by Kiderlen and Jensen [3] and it has been extended to  $n \times n$  configurations in [2]. Most of the concepts considered in the two-dimensional space  $\mathbb{R}^2$  and presented in [2] have their counterparts in  $\mathbb{R}^3$ . The theoretical discussion in the previous articles was based on the *model-based* approach, in which an anisotropic structure was represented as a stationary random set  $Z$ , extending over the entire space. The simpler *design-based* approach presented here assumes that  $Z$  is deterministic and bounded. This approach is often more appropriate for the analysis of biomedical images.

In Section 2 we will give a design-based definition of the oriented rose and introduce  $n \times n \times n$  configurations. In Section 3, it is shown how the probability of observing an  $n \times n \times n$  configuration is related to the oriented rose. Section 4 deals with informative configurations and twins. In particular, a geometric characterization of informative configurations is given and an algorithm for finding all  $n \times n \times n$  informative configurations is developed. Estimation of the oriented rose from  $2 \times 2 \times 2$  configuration counts is presented in Section 5. In Section 6, the approach is illustrated by two examples. The paper is concluded with some general remarks in Section 7

## 2 Background

### 2.1 The normal measure and the oriented rose

Let  $Z$  be a bounded subset of the three-dimensional space  $\mathbb{R}^3$ . We suppose that  $Z$  is a finite union of closed convex sets with interior points. This ensures that  $Z$  has finite surface area and a sufficiently smooth boundary  $\partial Z$  such that the part where a unique outer normal cannot be defined, has area zero. We also assume, that  $Z$  is contained in a closed bounded set  $Y \subseteq \mathbb{R}^3$ , called the reference space.

Let  $A$  be a set of directions in  $\mathbb{R}^3$ . (Formally,  $A$  is a measurable subset of the unit sphere  $S^2$  in  $\mathbb{R}^3$ .) Let  $N_Z(A)$  be the set of all boundary points of  $Z$  having an outer normal in  $A$ . The *normal measure*  $\mathcal{S}$  of  $Z$  with respect to  $Y$  is defined by

$$\mathcal{S}(A) = \frac{S(N_Z(A))}{V(Y)}, \quad (1)$$

where  $S$  denotes surface area and  $V$  denotes volume. If this measure is normalized, we get the *oriented rose of normal directions*

$$\mathcal{R}_o(A) = \frac{\mathcal{S}(A)}{\mathcal{S}(S^2)} = \frac{S(N_Z(A))}{S(\partial Z)}. \quad (2)$$

These definitions are in analogy with the corresponding notions in the stationary case, which can be found for example in Weil [8, 9]. Note that  $\mathcal{R}_o(A)$  can be interpreted as the probability that the outer unit normal at a uniform random point on  $\partial Z$  belongs to  $A$ . It can be shown that  $\mathcal{S}$  (and accordingly  $\mathcal{R}_o$ ) is always a centered measure, i.e.

$$\int_{S^2} u \mathcal{S}(du) = 0, \quad (3)$$

see [8, p. 395] for details.

## 2.2 $n \times n \times n$ configurations

We assume that the set  $Z$  is not observed directly, but only via a discretization, performed by means of a scaled lattice  $t\mathbb{L}$ , where  $t > 0$ ,

$$\mathbb{L} := \mathbb{Z}^3 = \{(i_1, i_2, i_3) \mid i_1, i_2, i_3 \in \mathbb{Z}\},$$

and  $\mathbb{Z}$  denotes the integers. The set  $Y \cap t\mathbb{L}$  corresponds to a 3D digital image; any of its points can be considered as a voxel. To each voxel a *brightness value* is associated. This brightness value belongs to a finite set of colors, referred to as the *palette*. In the considered case, voxels of  $Y \cap t\mathbb{L}$  belong either to  $Z \cap t\mathbb{L}$  or to  $Z^C \cap t\mathbb{L}$ , where  $Z^C := \mathbb{R}^3 \setminus Z$  is the complement of  $Z$ , i.e. the background of the image. Hence the palette consists of two elements, black and white ( $b$  and  $w$ , respectively). It is arbitrarily assumed that voxels belonging to  $Z \cap t\mathbb{L}$  have brightness value  $b$ , while the remaining voxels have value  $w$ .

In Jensen and Kiderlen [2], it is demonstrated how the oriented rose of a planar set  $Z$  can be estimated, using so-called configuration counts. We generalize this concept to 3D. Let

$$\mathbb{L}_n := \{(i_1, i_2, i_3) \mid i_1, i_2, i_3 = 0, \dots, n-1\} \subset \mathbb{L}$$

be the  $n$ -lattice cube. An  $n \times n \times n$  configuration is any 3D binary image on a scaled lattice cube  $t\mathbb{L}_n$ . Equivalently, we may think of a configuration as a subset  $tB$  of the scaled lattice cube  $t\mathbb{L}_n$  which consists of voxels having a brightness value  $b$ , or a pair  $(tB, tW)$ , where  $tW$  is complementary to  $tB$  in  $t\mathbb{L}_n$ . Wherever we consider a configuration without referring to its scaling factor,  $t$  will be omitted.

In the following, we recall a method to enumerate  $n \times n \times n$  configurations with the integers  $0, \dots, 2^{n^3} - 1$ . It was apparently first suggested by the Centre de Morphologie Mathématique in Fontainebleau (see Serra [7]). Details can also be found in Ohser and Mücklich [5]. First, the voxels of  $t\mathbb{L}_n$  are enumerated by assigning the integer  $k = k(p) := n^2 i_1 + n i_2 + i_3$  to the voxel  $p = t(i_1, i_2, i_3) \in t\mathbb{L}_n$ . Using the numbering of voxels, each of the  $2^{n^3}$  configurations of size  $n \times n \times n$  can be assigned a unique number. For the configuration  $tB$  this number is

$$N(tB) = \sum_{k=0}^{n^3-1} 2^k \cdot 1_{tB}(p_k), \quad (4)$$

where  $p_k \in t\mathbb{L}_n$  is the voxel with associated number  $k$ .

Configurations different from  $\emptyset$  and  $t\mathbb{L}_n$  are called *boundary configurations*, as they contain information about the boundary of  $Z$ .

### 3 The probability of observing an $n \times n \times n$ configuration

#### 3.1 An asymptotic result for large resolution

Kiderlen and Jensen in [3] proved a formula for the asymptotic probability of observing different  $n \times n$  configurations in a planar binary image. In the theorem below, we formulate and prove a corresponding 3-dimensional result. In contrast to the model-based approach used in [3], we here take a design-based point of view.

Consider the random experiment of translating a scaled version  $t\mathbb{L}_n$  uniformly in  $Y$ , such that the translated scaled lattice cube hits  $Y$ . Thus we consider  $t\mathbb{L}_n + x_t$ , where  $x_t$  is a uniform random point in

$$X_t = \{x \in \mathbb{R}^3 \mid (t\mathbb{L}_n + x) \cap Y \neq \emptyset\}. \quad (5)$$

Since  $(t\mathbb{L}_n + x) \cap Y \neq \emptyset$  if and only if there exists  $y \in Y$  and  $z \in t\mathbb{L}_n$  such that  $x = y - z$ , we have

$$X_t = \{y - z \mid y \in Y, z \in t\mathbb{L}_n\}. \quad (6)$$

The probability that in the randomly translated scaled lattice cube  $t\mathbb{L}_n + x_t$  we observe the configuration  $(tB, tW)$  is

$$P(tB + x_t \subset Z, tW + x_t \subset Z^C).$$

In Theorem 1 below, a formula for this probability, valid for small  $t$ , is given. The probability depends on the normal measure and the function  $h_{(B,W)}$  defined by

$$h_{(B,W)}(v) := \left[ \min_{w \in W} \langle w, v \rangle - \max_{b \in B} \langle b, v \rangle \right]^+, \quad v \in S^2, \quad (7)$$

with  $f^+ := \max\{0, f\}$  denoting the positive part of a function  $f$  and

$$\langle x, y \rangle := x_1y_1 + x_2y_2 + x_3y_3$$

being the usual scalar product of the vectors  $x = (x_1, x_2, x_3)$  and  $y = (y_1, y_2, y_3)$  in  $\mathbb{R}^3$ . The function  $h_{(B,W)}$  evaluated at  $v \in S^2$  has a nice geometric interpretation: consider a plane  $p$  with normal  $v$ . Let  $H^+$  and  $H^-$  be the positive and negative closed half-spaces of  $p$ . Then,  $h_{(B,W)}(v)$  is the width of the strip  $S_v$  of all such planes with  $B \subset H^-$  and  $W \subset H^+$ , cf. Figure 1. If  $S_v$  is empty, its width is considered to be 0, so  $h_{(B,W)}(v) = 0$  in this case.

**Theorem 1** *For any 3D boundary configuration  $(tB, tW)$  we have*

$$\lim_{t \rightarrow 0^+} \frac{1}{t} P(tB + x_t \subset Z, tW + x_t \subset Z^C) = \int_{S^2} h_{(B,W)}(v) d\mathcal{S}(v). \quad (8)$$

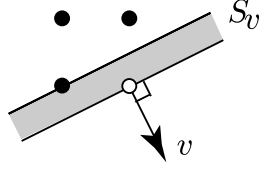


Figure 1: 2D illustration of the geometric interpretation of the function  $h_{(B,W)}$ . For details, see text.

The proof of this theorem can be found in Appendix A. Theorem 1 connects the probability to observe a boundary configuration  $(tB, tW)$  to a certain integral with respect to the normal measure. Clearly, only those configurations yield information on  $\mathcal{S}$ , for which  $h_{(B,W)}$  is not identical to 0 on  $S^2$ . Boundary configurations with this property are therefore called *informative configurations*. In other words,  $(B, W)$  is an informative configuration if and only if there is  $v \in S^2$  such that the strip  $S_v$  has a positive width, cf. Figure 1. This is equivalent to saying that there is a plane  $p$  with normal  $v$  strictly separating  $B$  and  $W$  (i.e.  $B$  lies on one side of  $p$ ,  $W$  lies on the other side of  $p$  and  $p \cap (B \cup W) = \emptyset$ ). Thus  $(B, W)$  is informative if and only if  $B$  and  $W$  can be strictly separated by a plane.

### 3.2 Estimation from binary images

In applications, replicated generation of a uniformly translated lattice cube  $t\mathbb{L}_n + x_t$  is performed. Usually, independent replication is impracticable and a systematic scheme is more appropriate. In order to explain this in more detail, recall that the feature of interest is  $Z$ , contained in the reference space  $Y$ . In applications, a specimen  $X \subseteq Y$  is available for examination, cf. Figure 2.

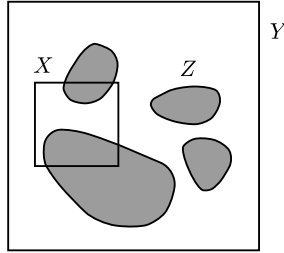


Figure 2: Illustration of the restricted and extended cases. The feature of interest  $Z$  is contained in the reference space  $Y$ . The specimen available for examination is  $X$ . In the restricted case  $X = Y$ , while in the extended case  $X$  is a part of  $Y$ .

Two cases should be distinguished, cf. Miles [4]. In the *restricted case*, the specimen  $X$  is the whole reference space  $Y$ , e.g.  $X$  is a whole organ or tumor. In this case, it is natural to use an unbounded cubic lattice with uniform position. Let  $z$  be a uniform random vector in  $[0, 1]^3$ . For a given configuration  $(B, W)$ , the ratio

$$\frac{\sum_{i \in \mathbb{L}} 1\{t(B + z + i) \subset Z, t(W + z + i) \subset Z^c\}}{\sum_{i \in \mathbb{L}} 1\{t(\mathbb{L}_n + z + i) \cap Y \neq \emptyset\}} \quad (9)$$

can be determined from the digitization: The numerator is just the number of  $(B, W)$ -configurations of the digitization  $Z \cap t(\mathbb{L} + z)$ . It is divided by the number of (scaled)  $n \times n \times n$  lattice cubes hitting  $Y$ . A standard argument shows that (9) is a ratio-unbiased estimator for

$$\mathbb{P}(tB + x_t \subset Z, tW + x_t \subset Z^C). \quad (10)$$

Instead of the observation of configurations in all  $n \times n \times n$  lattice cubes, a systematic subset of these lattice cubes can be considered. Note that this procedure is free of edge effects, as an unbounded lattice is used here.

In the *extended case*, the specimen  $X$  available for examination is but a portion of the much larger reference space  $Y$ . If the specimen  $X$  is cuboidal, a digitization of  $X$  will be a discrete scaled cuboidal window  $tD$ , where

$$D = \{0, \dots, k-1\} \times \{0, \dots, l-1\} \times \{0, \dots, m-1\},$$

say. Let us suppose that  $tD$  is uniformly translated in  $Y$ , such that part of the translated  $tD$  hits  $Y$ . Contained in this uniformly scaled cuboidal window are

$$(k-n+1)(l-n+1)(m-n+1)$$

scaled  $n \times n \times n$  lattice cubes, each being uniform in a set containing  $X_t$ . For each of these cubes, Theorem 1 still holds. Thus, the relative number of a configuration  $(B, W)$  in  $tD$  is an unbiased estimator for the probability (10). Ohser & Mücklich [5, p. 111] mention that this procedure is free of edge effects as it is based on observations in a reduced window.

## 4 Twins and informative configurations

For certain configurations  $(B, W)$  the corresponding functions  $h_{(B,W)}$  coincide. As in the planar case, we introduce a *twin pair* configuration  $(B, W)^*$  of  $(B, W)$ . It is  $(B, W)^* := (B', W')$  with

$$B' := \rho_n(W), \quad W' := \rho_n(B),$$

where  $\rho_n$  denotes the reflection of a set at the midpoint  $(\frac{n-1}{2}, \frac{n-1}{2}, \frac{n-1}{2})$  of  $\mathbb{L}_n$ . If the process of finding a twin results in the original configuration, we call it a *self-twin*. From the definitions of  $h_{(B,W)}$  and the twin pair, it follows that

$$h_{(B,W)^*} = h_{(B,W)}.$$

The total number of  $n \times n \times n$  configurations is  $2^{n^3}$ . The crucial task is to determine the set of informative configurations, since only these configurations have asymptotically non-vanishing probabilities of being observed. As the three dimensional problem is slightly more involved than the planar one, we recall the latter for comparison. Recall the following definition of separation in general dimension:

two subsets of (the  $d$ -dimensional space)  $\mathbb{R}^d$  can be separated if there is a hyperplane such that the two corresponding closed half spaces contain one of the sets, each. The sets can be strictly separated if the separating hyperplane can be chosen such that it does not hit any of the two sets. Lemma 1 in [2] states that two planar subsets  $B$  and  $W$  of the  $n \times n$ -lattice square can be separated if and only if there exists an  $n$ -lattice line separating  $B$  and  $W$  and not hitting both of them. Here, an  $n$ -lattice line in the plane is a line passing through at least two points of the  $n \times n$ -lattice square. This lemma has been the basis for an algorithm for searching all planar informative configurations [2]. However, Lemma 1 cannot be directly modified by replacing lines with planes. The algorithm of searching 3D configurations is instead based on Proposition 2 below. For its formulation we need the notion of an  $n$ -lattice plane, which is a plane in  $\mathbb{R}^3$  passing through at least 3 points of  $\mathbb{L}_n$ , see Figure 3, left, for an illustration.

**Proposition 2** For a boundary configuration  $(B, W)$  in  $\mathbb{L}_n$  the following two statements are equivalent:

- (i)  $(B, W)$  is informative.
- (ii) The two sets  $B$  and  $W$  can be separated by an  $n$ -lattice plane  $p_n$  such that if  $p_n$  hits both sets, there is an  $n$ -lattice line  $g_n \subset p_n$  separating  $B \cap p_n$  and  $W \cap p_n$ , only hitting one of them.

Condition (ii) of this proposition is illustrated in Figure 3. A proof is given in Appendix A.

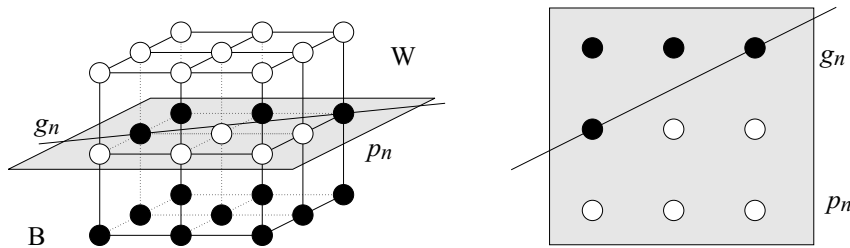


Figure 3: Illustration of condition (ii) of Proposition 2. On the left, a  $3 \times 3 \times 3$  configuration  $(B, W)$  is shown. The separating  $n$ -lattice plane  $p_n$  hits both,  $B$  and  $W$ . On the right hand side, the intersection of the configuration with  $p_n$  is indicated: as  $g_n$  is a separating  $n$ -lattice line in  $p_n$  not hitting  $W$ , condition (ii) of Proposition 2 is satisfied.

Proposition 2 enables us to formulate the following algorithm of searching all informative 3D configurations. The informative configurations are collected in the set  $T_n$ .

### Algorithm 1

1. Set  $T_n := \emptyset$ .
2. Choose an  $n$ -lattice plane  $p_n$ . Decompose  $\mathbb{L}_n$  into the three sets  $L$ ,  $L^+$  and  $L^-$ , where  $L = \mathbb{L}_n \cap p_n$ , and  $L^+$  and  $L^-$  are the remaining points of  $\mathbb{L}_n$ , lying on different sides of  $p_n$ .
3. Choose two lattice points on  $p_n$  and let  $g_n$  be the line passing through them.
4. Decompose  $L$  into  $G = g_n \cap \mathbb{L}_n$ ,  $G^+$  and  $G^-$ , where  $G^+$  and  $G^-$  are the remaining points in  $L$  on each side of  $g_n$ .
5. Put  $W = L^-$  and  $B = L^+$  and then, successively,
  - (a) Put  $W = W \cup G^-$  and  $B = B \cup G^+ \cup G$
  - (b) Put  $W = W \cup G^- \cup G$  and  $B = B \cup G^+$
  - (c) Put  $W = W \cup G^+$  and  $B = B \cup G^- \cup G$
  - (d) Put  $W = W \cup G^+ \cup G$  and  $B = B \cup G^-$For each of (a),  $\dots$ , (d) include  $(B, W)$  in  $T_n$ , if both  $B$  and  $W$  are nonempty.
6. Repeat 5 with  $W = L^+$  and  $B = L^-$ .
7. Go to 3 and pick another pair of points until all lattice lines in  $p_n$  have been analysed.
8. Go to 2 and pick another  $n$ -lattice plane until all  $n$ -lattice planes have been analysed.
9. The output  $T_n$  is the set of all informative  $n \times n \times n$  configurations.

For  $n = 2$  it is easy to try out all the  $2^{2^3} = 256$  configurations without using Algorithm 1. However, Algorithm 1 is helpful in the case  $n \geq 3$ , because the number of *all*  $n \times n \times n$  configurations increases exponentially in  $n$ . For reference, we list in Appendix B all informative  $2 \times 2 \times 2$  configurations.

## 5 Implementation

In the following, an estimation procedure is discussed for the case  $n = 2$ . We approximate  $\mathcal{S}$  by a discrete measure  $\widehat{\mathcal{S}}$ , supported by the directions  $v_1, \dots, v_{26}$  determined by all ordered pairs of vertices of the unit cube. Among all informative  $2 \times 2 \times 2$  configurations, there are 54 configurations  $(B, W)$  not having all values  $h_{(B,W)}(v_j)$ ,  $j = 1, \dots, 26$ , equal to 0. Moreover, for each such configuration  $h_{(B,W)}(v_j) > 0$  holds for only one  $v_j$ . If two configurations among the 54 have positive  $h$ -value

for the same direction, their value is identical. Therefore it is possible to partition these 54 configurations into 26 classes, each class associated with one vector  $v_m$ ,  $m = 1, \dots, 26$ .

Table 1 presents these 54 configurations partitioned according to such vectors. The configurations are ordered according to increasing configuration number. The common value  $h_m = h_{(B,W)}(v_m)$  for all configurations  $(B, W)$  belonging to class  $m$  is also given. For the sake of legibility, here and further on all the vectors corresponding to normal directions will be presented as unnormalised. Note that two configurations  $(B, W)$  and  $(B', W')$ , belonging to the same class, do not necessarily have identical  $h$  functions. For instance, consider class 1 and direction  $v = [0.5, 0.5, 1]$ . For configuration 1,  $h_{B,W}(v) = \frac{1}{\sqrt{6}}$ , while for configuration 23,  $h_{B,W}(v) = 0$ .

Table 1: The 26 classes of 54 configurations. 's' indicates that the configuration is a self-twin.

class no. m	vector $v_m$	config. $N$	twin $N$	config. $N$	twin $N$	$h_m$
1	$[1, 1, 1]$	 1	 127	 23	s	$\frac{\sqrt{3}}{3}$
2	$[1, 1, -1]$	 2	 191	 43	s	$\frac{\sqrt{3}}{3}$
3	$[1, 1, 0]$	 3	 63	—	—	$\frac{\sqrt{2}}{2}$
4	$[1, -1, 1]$	 4	 223	 77	s	$\frac{\sqrt{3}}{3}$
5	$[1, 0, 1]$	 5	 95	—	—	$\frac{\sqrt{2}}{2}$
6	$[1, -1, -1]$	 8	 239	 142	s	$\frac{\sqrt{3}}{3}$
7	$[1, 0, -1]$	 10	 175	—	—	$\frac{\sqrt{2}}{2}$
8	$[1, -1, 0]$	 12	 207	—	—	$\frac{\sqrt{2}}{2}$

*continues*

Table 1: (continued)

class no. m	vector $v_m$	config. $N$	twin $N$	config. $N$	twin $N$	$h_m$
9	$[1, 0, 0]$	 15	s	—	—	1
10	$[-1, 1, 1]$	 16	 247	 113	s	$\frac{\sqrt{3}}{3}$
11	$[0, 1, 1]$	 17	 119	—	—	$\frac{\sqrt{2}}{2}$
12	$[-1, 1, -1]$	 32	 251	 178	s	$\frac{\sqrt{3}}{3}$
13	$[0, 1, -1]$	 34	 187	—	—	$\frac{\sqrt{2}}{2}$
14	$[-1, 1, 0]$	 48	 243	—	—	$\frac{\sqrt{2}}{2}$
15	$[0, 1, 0]$	 51	s	—	—	1
16	$[-1, -1, 1]$	 64	 253	 212	s	$\frac{\sqrt{3}}{3}$
17	$[0, -1, 1]$	 68	 221	—	—	$\frac{\sqrt{2}}{2}$
18	$[-1, 0, 1]$	 80	 245	—	—	$\frac{\sqrt{2}}{2}$
19	$[0, 0, 1]$	 85	s	—	—	1
20	$[-1, -1, -1]$	 128	 254	 232	s	$\frac{\sqrt{3}}{3}$

*continues*

Table 1: (continued)

class no. m	vector $v_m$	config. $N$	twin $N$	config. $N$	twin $N$	$h_m$
21	$[0, -1, -1]$	136	238	—	—	$\frac{\sqrt{2}}{2}$
22	$[-1, 0, -1]$	160	250	—	—	$\frac{\sqrt{2}}{2}$
23	$[0, 0, -1]$	170	s	—	—	1
24	$[-1, -1, 0]$	192	252	—	—	$\frac{\sqrt{2}}{2}$
25	$[0, -1, 0]$	204	s	—	—	1
26	$[-1, 0, 0]$	240	s	—	—	1

Let  $k_m$  be the number of configurations in class  $m$ ,  $m = 1, \dots, 26$ ; for instance  $k_1 = 3$  and  $k_9 = 1$ . We refer to  $p_m$  as the probability of observing a configuration in class  $m$ . The probability  $p_m$  can be estimated from replicated observation, as explained at the end of Section 3. If  $n_m$  denotes the number of observed configurations in class  $m$ , then

$$\hat{p}_m = \frac{n_m}{n_{total}},$$

where  $n_{total}$  is the total number of observed, not only informative,  $2 \times 2 \times 2$  configurations.

A reasonable requirement for  $\hat{\mathcal{S}}$  to be an estimator of  $\mathcal{S}$  is that (8) should hold true for  $\hat{\mathcal{S}}$  in place of  $\mathcal{S}$ . Hence,

$$p_m = tk_m h_m \hat{\mathcal{S}}(\{v_m\}), \quad m = 1, \dots, 26. \quad (11)$$

should hold approximately and we define the mass of  $\hat{\mathcal{S}}$  in  $v_m$  by

$$\hat{\mathcal{S}}(\{v_m\}) := \frac{\hat{p}_m}{tk_m h_m}, \quad m = 1, \dots, 26. \quad (12)$$

Note that in contrast to the planar case in [2] the constraint (3) is not taken into account in this procedure. The advantages of omitting this constraint are that firstly, the estimation procedure is straightforward and secondly, that it can easily be extended to multiphase materials: Consider a material consisting of three (or more) phases, say of red, blue and yellow color. Our procedure can be used to estimate the distribution of the normal pointing from red to blue (not regarding the yellow phase), say. This distribution will not satisfy (3) in general.

On the other hand, there is also an advantage to take (3) into account as the resulting estimator can then be illustrated by a set in three-dimensional space. The procedure is then as follows: Informally, we have to find a measure  $\tilde{\mathcal{S}}$  supported by  $\{v_1, \dots, v_{26}\}$ , such that  $\tilde{\mathcal{S}}(\{v_m\})$  fits 'best possible' to the measurements  $\frac{\hat{p}_m}{tk_m h_m}$  under the constraint that  $\tilde{\mathcal{S}}$  is centered. The estimator then can be interpreted as the surface area measure of a centered compact convex set  $\tilde{B}(Z)$  (this means that the two-dimensional facets of  $\tilde{B}(Z)$  have outer unit normals  $v_m$  and area  $\tilde{\mathcal{S}}(\{v_m\})$ ,  $m = 1, \dots, 26$ ). The set  $\tilde{B}(Z)$  is called the *estimated Blaschke body* of  $Z$  and represents the estimated directional information more intuitively than a discrete measure. The use of associated sets (often called associated convex bodies) to geometric structures  $Z$  is well established in stochastic geometry: In the case, where  $Z$  is a (stationary) random closed set, associated bodies are introduced and studied e.g. in [8] and in the book [6, Kapitel 4.5].

We describe now in more detail the estimation procedure to obtain  $\tilde{B}(Z)$ . In a first step the above mentioned constrained optimization problem to find the masses  $\theta_m = \tilde{\mathcal{S}}(\{v_m\})$ ,  $m = 1, \dots, 26$ , must be formalized. The constraint (3) for  $\tilde{\mathcal{S}}$  reads

$$\sum_{i=1}^{26} \theta_m v_m = 0. \quad (13)$$

Following the two-dimensional case in [3] and [2], we suggest to choose  $\theta = (\theta_1, \dots, \theta_{26})$  to be a solution of the problem

$$\begin{aligned} & \text{maximize } \ell(\theta) = \sum_{m=0}^{26} n_m \ln p_m(\theta) \\ & \text{subject to (13) and } \theta \geq 0. \end{aligned} \quad (14)$$

Here, according to (11),  $p_m(\theta) = tk_m h_m \theta_m$ ,  $m = 1, \dots, 26$ . We set

$$p_0(\theta) = 1 - \sum_{m=1}^{26} p_m(\theta) \quad \text{and} \quad n_0 = n_{total} - \sum_{m=1}^{26} n_m$$

to take into account the number of all non-informative configurations. One reason for the choice of the objective function  $\ell(\theta)$  is the fact that its maximization leads to a maximum likelihood estimator of  $\theta$  in the (hypothetical) case of independent observations (see [3] for more details on  $\ell(\theta)$ ). As (14) is a convex optimization problem, it can be solved with standard software. Once  $\tilde{\mathcal{S}}$  is found, the algorithm in [1] can be used to find the estimated Blaschke body  $\tilde{B}(Z)$  corresponding to  $\tilde{\mathcal{S}}$ .

In the next section we give two simple simulation examples to illustrate the estimation procedure.

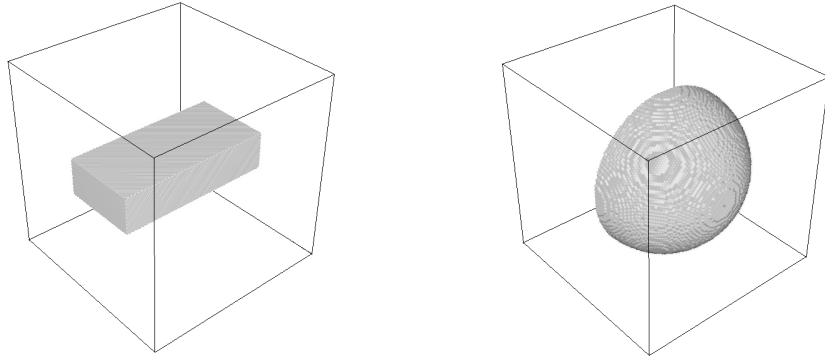


Figure 4: The two simulation examples: cuboid and hemisphere contained in  $Y$ .

## 6 Examples

### *Cuboid with axes-parallel edges*

The 3D image contains a single cuboid  $Z \subset Y$ , cf. Figure 4, left. The dimensions of the reference space  $Y$  are  $125 \times 125 \times 125$ , and the dimensions of the cuboid are  $100 \times 50 \times 25$ . The normal measure is known for this image. It can be found by calculating the area of each face and normalizing it with respect to the volume of the image, being  $V = 125^3$ .

The image was analyzed, using a resolution of  $1/t = 1$ . Only 3% of the total mass of the estimated measure were not concentrated at the 6 normal directions of the cuboid. Table 2 compares the true and estimated values of the oriented rose. As these values correspond (approximately) to a centered measure, the two estimators  $\hat{\mathcal{S}}$  and  $\tilde{\mathcal{S}}$  coincide. The estimated masses at these 6 directions correspond to an estimated Blaschke body, which is a cuboid of side lengths  $93.8 \times 49.8 \times 24.4$ .

Table 2: Comparison of the normal measure calculated directly and estimated from the 3D binary image of the cuboid

normal vector	surface area of the corresponding face	exact normal measure $\mathcal{S}$ of $Z$	estimated normal measure $\hat{\mathcal{S}} = \tilde{\mathcal{S}}$
$[0, 0, 1]$	5000	2.56	2.39
$[0, 0, -1]$	5000	2.56	2.39
$[0, 1, 0]$	2500	1.28	1.17
$[0, -1, 0]$	2500	1.28	1.17
$[1, 0, 0]$	1250	0.64	0.62
$[-1, 0, 0]$	1250	0.64	0.62
others	0	0	0.25

*Hemisphere* The reference space  $Y$  (size  $125 \times 125 \times 125$ ) contains a single solid

Table 3: The masses ( $\ast 10^4$ ) of the estimators  $\widehat{\mathcal{S}}$  and  $\widetilde{\mathcal{S}}$  in the example of the hemisphere.

vector	$\widehat{\mathcal{S}}$	$\widetilde{\mathcal{S}}$	vector	$\widehat{\mathcal{S}}$	$\widetilde{\mathcal{S}}$
[ 0, 0, 1]	3.20	3.20	[ 1, 1,-1]	5.82	6.09
[ 0, 0,-1]	3.20	3.20	[ 1,-1, 0]	0.14	0.14
[ 0, 1, 0]	6.39	7.40	[ 1,-1, 1]	0.09	0.17
[ 0, 1, 1]	4.83	5.19	[ 1,-1,-1]	0.09	0.17
[ 0, 1,-1]	4.83	5.19	[-1, 0, 0]	3.20	3.20
[ 0,-1, 0]	40.00	35.33	[-1, 0, 1]	2.42	2.42
[ 0,-1, 1]	0.14	0.14	[-1, 0,-1]	2.42	2.42
[ 0,-1,-1]	0.14	0.14	[-1, 1, 0]	4.84	5.19
[ 1, 0, 0]	3.20	3.20	[-1, 1, 1]	5.82	6.09
[ 1, 0, 1]	2.42	2.42	[-1, 1,-1]	5.82	6.09
[ 1, 0,-1]	2.42	2.42	[-1,-1, 0]	0.15	0.14
[ 1, 1, 0]	4.83	5.19	[-1,-1, 1]	0.09	0.17
[ 1, 1, 1]	5.82	6.09	[-1,-1,-1]	0.09	0.17

hemisphere  $Z$  with radius  $r = 50$ , cf. Figure 4, right. The unit normal vector of the circular flat face is  $v_0 = [0, -1, 0]$ . Notice that the normal measure of  $Z$  is given by

$$\mathcal{S}(A) = \frac{1}{V(Y)} [\pi r^2 1_A(v_0) + r^2 \int_{S_+^2} 1_A(v) dv], \quad (15)$$

where

$$S_+^2 = \{v \in S^2 \mid v = (v_1, v_2, v_3), v_2 \geq 0\}. \quad (16)$$

The image was analyzed using a resolution of  $1/t = 1$ . In contrast to the example of the cuboid, the normal measure is not concentrated on  $\{v_1, \dots, v_{26}\}$ . Hence, a direct comparison of the estimator  $\widehat{\mathcal{S}}$  with the normal measure of  $Z$  is not possible. The measure  $\widehat{\mathcal{S}}$  is not centered and therefore differs from the second estimator  $\widetilde{\mathcal{S}}$ , the latter being centered by definition. In Table 3 the masses of the two estimators are listed for comparison. Both estimators show a clear maximum in the direction  $[0, -1, 0]$ , which is due to the large number of observations of boundary configurations hitting the flat face of  $Z$ . The measure  $\widetilde{\mathcal{S}}$  can be represented using the estimated Blaschke body  $\widetilde{B}(Z)$ . This body is shown in Figure 5; it is a polyhedral approximation of the hemisphere.

According to Theorem 1, non-informative boundary configurations (i.e. non-informative configurations that are not monochrome) cannot occur asymptotically, but they occur with positive probability if we work with finite resolution (and if the feature of interest has “non-convex corners”). A large relative number  $\xi$  of observations of non-informative boundary configurations indicates that the resolution is not sufficiently high compared to the features of  $Z$ . In [2], as a rule of thumb for the planar case, it has been suggested to consider the resolution to be sufficient if  $\xi$  is below 1%. In the spatial case, a similar benchmark could be used.

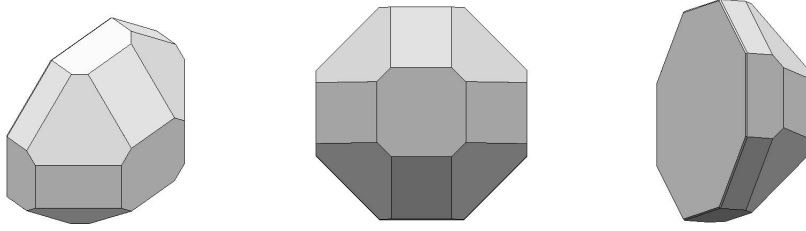


Figure 5: The estimated Blaschke body  $\tilde{B}(Z)$  seen from different viewpoints. On the left, the perspective corresponds to Figure 4, right.

## 7 Discussion

The extension of the planar method proposed in [3, 2] to three dimensional space can be a useful tool in estimation of the directional distributions of spatial structures  $Z$ . Our method allows to find a discrete estimator of this measure, based on a configuration analysis of a discretization of  $Z$ .

However, there is still room for future improvements of the present implementation. It should be emphasized that the estimation procedure in Section 5 does not use the complete information of all informative  $2 \times 2 \times 2$  configurations. We have chosen a proper subset of all informative configurations because then the estimated masses  $\hat{\mathcal{S}}(\{v_m\})$  have a straightforward interpretation in terms of the frequency of class- $m$ -configurations,  $m = 1, \dots, 26$ , as expressed in (12). A more detailed study would use *all* 102 informative configurations, as listed in Table 4, Appendix B. formed by twins.

The estimation procedure presented here is based on the asymptotic result of Theorem 1, which holds as  $t$  becomes arbitrarily small i.e. the resolution  $1/t$  becomes large. In applications, however, one is forced to work with (one or several) fixed scaling factors  $t$  and the resulting estimator clearly depends on  $t$ . Since the estimator of the mean normal measure  $\hat{\mathcal{S}}$  given by (12), depends linearly on the configuration counts, this dependence on  $t$  is continuous, meaning that for small  $t$  the estimator is close to the true normal measure, if the latter satisfies the model. An additional difficulty in applications is the presence of noise in the digitized image. Clearly, configuration counts are sensitive to noise and its effect on the estimators is an interesting question that will be considered in future work.

**Acknowledgements** We want to thank two colleagues for their very friendly help with the second simulation example: Kim Allan Andersen solved (14) numerically and Richard Gardner reconstructed the estimated Blaschke body  $\tilde{B}(Z)$  from  $\tilde{\mathcal{S}}$ .

This research was done while the first author was a Marie Curie fellow at the Marie Curie training site Advanced Medical Imaging and Spatial Statistics. This work has been supported in part by the Danish Natural Science Research Council and

MaPhySto – Network in Mathematical Physics and Stochastics, funded by the Danish National Research Foundation.

## References

- [1] Gardner, R. J., Milanfar, P. (2003), Reconstruction of convex bodies from brightness functions, *Disc. Comput. Geom.* 29, 279–303.
- [2] Jensen, E.B.V., Kiderlen, M. (2003), Directional analysis of digitized planar sets by configuration counts, *J. Microsc.* 212, 158–168.
- [3] Kiderlen, M., Jensen, E.B.V. (2003), Estimation of the directional measure of planar sets by digitization, *Adv. Appl. Prob.* 35, 583–602.
- [4] Miles, R. E. (1978), The importance of proper model specification in stereology, in: *Geometric Probability and Biological Structures: Buffon's 200th Anniversary*, (R. E. Miles and J. Serra, eds.) Lecture Notes in Biomathematics, Vol. 23, Springer, Berlin, 115–136.
- [5] Ohser, J., Mücklich, F. (2000), *Statistical Analysis of Microstructures in Material Science*, Wiley, New York.
- [6] Schneider, R., Weil, W. (2000) *Stochastische Geometrie*, Teubner, Stuttgart.
- [7] Serra, J. (1969), Introduction à la Morphologie Mathématique, *Cahiers du Centre de Morphologie Mathématique*, Booklet no. 3 ENSMP, Fontainebleau.
- [8] Weil, W. (1997), Mean bodies associated with random closed sets, *Suppl. Rend. Circ. Mat. Palermo*, (2) 50, 387–412.
- [9] Weil, W. (1997), The mean normal distribution of stationary random sets and particle processes, in: *Advances in Theory and Applications of Random Sets, Proc. Internat. Symp., Oct. 9-11, 1996, Fontainebleau, France*, (D. Jeulin, ed.) World Scient. Publ., Singapore, 21–33.

## Appendix A: Proofs.

In this appendix, we give proofs of Theorem 1 and Proposition 2.

### (Heuristic) proof of Theorem 1:

Let  $Z$  be a finite union of closed convex sets with interior points contained in the reference space  $Y$ , and let  $(tB, tW)$  be a 3D boundary configuration with scaling factor  $t > 0$ .

Since  $x_t$  is uniform in  $X_t$ , given by (5), we have

$$P(tB + x_t \subset Z, tW + x_t \subset Z^C) = \frac{V(\Lambda_{(tB, tW)})}{V(X_t)},$$

where  $\Lambda_{(tB, tW)}$  is the set of all translation vectors  $x \in X_t$  for which  $t\mathbb{L}_n + x$  produces the configuration  $(tB, tW)$ . Since  $tB + x \subset Z$  implies that  $(t\mathbb{L}_n + x) \cap Y \neq \emptyset$  we can allow arbitrary translations and put

$$\Lambda_{(tB, tW)} = \{x \in \mathbb{R}^3 \mid tB + x \subset Z, tW + x \subset Z^C\}.$$

The boundary of  $Z$  can locally be thought to be a small disc  $dz$  in a plane  $p$ . Let  $v$  be the outer unit normal of  $Z$  at that plane  $p$ . We call  $x \in \mathbb{R}^3$  a ‘local translation’ if the cube  $t[0, n-1]^3 + x$  hits the disc. For sufficiently small  $t > 0$ , the volume of the set of local translations  $x \in \mathbb{R}^3$  with  $tB + x \subset Z$  and  $tW + x \subset Z^C$  is approximately

$$t h_{(B,W)}(v) dz. \tag{17}$$

Integration over the surface  $\partial Z$  corresponds to integration on  $S^2$  with respect to the surface area measure  $S(\partial Z)\mathcal{R}_0$ . Hence, for small  $t > 0$  we have

$$\begin{aligned} P(tB + x_t \subset Z, tW + x_t \subset Z^C) &\approx \frac{t \int_{S^2} h_{(B,W)}(v) S(\partial Z) d\mathcal{R}_o(v)}{V(X_t)} \\ &= t \frac{V(Y)}{V(X_t)} \int_{S^2} h_{(B,W)}(v) d\mathcal{S}(v). \end{aligned}$$

As  $\lim_{t \rightarrow 0^+} V(X_t) = V(Y)$ , the assertion follows.  $\square$

It should be noted that the proof given above is heuristic since the local considerations leading to (17) are applied independently to every boundary point  $z$  of  $Z$ .

### Proof of Proposition 2:

We have already remarked after Theorem 1, that a configuration  $(B, W)$  is informative if and only if there is a plane strictly separating  $B$  and  $W$ .

”(i) implies (ii)”: Let us assume that there exists a plane  $p$  strictly separating  $B$  and  $W$  such that  $B \subset H^+$  and  $W \subset H^-$ , where  $H^+$  and  $H^-$  are the closed half-spaces associated to  $p$ . As  $p$  does not hit  $B \cup W$ , we can move the plane  $p$  to obtain an  $n$ -lattice plane as follows: Translation of  $p$  along its normal leads to a first intersection point with  $\mathbb{L}_n$ . If the resulting plane hits  $\mathbb{L}_n$  in one point only, it can be rotated

around this intersection point until it first hits  $\mathbb{L}_n$  in a second point. This leads to a separating plane having at least two points with  $\mathbb{L}_n$  in common. If there are precisely two points, a rotation around the axis given by these two points leads to a first intersection point with  $\mathbb{L}_n$  outside the rotation axes. The resulting plane is clearly an  $n$ -lattice plane  $p_n$ . The plane  $p_n$  separates  $B$  and  $W$  because none of the voxels has passed through the moved plane to the other side. If  $p_n$  is parallel to  $p$ , the rotation equals the identity and  $p_n$  is entirely contained in  $H^+$  or  $H^-$  and hence  $B \cap p_n = \emptyset$  or  $W \cap p_n = \emptyset$ . If  $p_n$  is not parallel to  $p$ , then the line  $g = p \cap p_n$  strongly separates  $B \cap p_n$  and  $W \cap p_n$  in  $p_n$ . As  $p_n$  contains at least 3 points of  $\mathbb{L}_n$ , a suitable translation and rotation of  $g$  in  $p_n$  leads to an  $n$ -lattice line separating  $B \cap p_n$  and  $W \cap p_n$  and not hitting both of them.

”(ii) implies (i)”: Let  $p_n$  be an  $n$ -lattice plane separating  $B$  and  $W$ . If  $B \cap p_n = \emptyset$  or  $W \cap p_n = \emptyset$  the assertion is clear as  $p_n$  can be suitably translated into a strictly separating plane. Assume therefore that  $B \cap p_n \neq \emptyset$ ,  $W \cap p_n \neq \emptyset$  and that  $g_n \subset p_n$  is an  $n$ -lattice line separating  $B \cap p_n$  and  $W \cap p_n$  in  $p_n$ , not hitting both of them. By a sufficiently small rotation of  $p_n$  around  $g_n$  we obtain a separating plane only hitting one of the sets  $B$  and  $W$ . Again, a suitable translation yields the assertion.  $\square$

## Appendix B

Table 4: All  $2 \times 2 \times 2$  informative configurations

No.	config.	$N$	twin	$N$
1		1		127
2		2		191
3		3		63
4		4		223
5		5		95
6		7		31
7		8		239
8		10		175
9		11		47
10		12		207
11		13		79
12		14		143
13		15	s	—
14		16		247
15		17		119
16		19		55
17		21		187

*continues*

Table 4: (continued)

No.	config.	$N$	twin	$N$
18		23	s	—
19		32		251
20		34		187
21		35		59
22		42		171
23		43	s	—
24		48		243
25		49		115
26		50		179
27		51	s	—
28		64		253
29		68		221
30		69		93
31		76		205
32		77	s	—
33		80		245
34		81		117

*continues*

Table 4: (continued)

No.	config.	$N$	twin	$N$
35		84		213
36		85	s	—
37		112		241
38		113	s	—
39		128		254
40		136		238
41		138		174
42		140		206
43		142	s	—
44		160		250
45		162		186
46		168		234
47		170	s	—
48		176		242
49		178	s	—
50		192		252
51		196		220

*continues*

Table 4: (continued)

No.	config.	$N$	twin	$N$
52		200		236
53		204	s	—
54		208		244
55		212	s	—
56		224		248
57		232	s	—
58		240	s	—